Optimal transport of cold atoms by modulating the velocity of traps*

Han Jing-Shan(韩景珊), Xu Xin-Ping(许忻平), Zhang Hai-Chao(张海潮)†, and Wang Yu-Zhu(王育竹)‡

Key Laboratory for Quantum Optics, Center for Cold Atom Physics, Shanghai Institute of Optics and Fine Mechanics, Chinese Academy of Sciences, Shanghai 201800, *China*

(Received 15 June 2012; revised manuscript received 30 July 2012)

This work experimentally demonstrates a new method of optimizing the transport of cold atoms via modulating the velocity profile imposed on a magnetic quadrupole trap. The trap velocity and corresponding modulation are controlled by varying the currents of two pairs of anti-Helmholtz coils. Cold ^{87}Rb atoms are transported in a non-adiabatic regime over 22 mm in 200 ms. For the transported atoms their final-vibration amplitude dependences of modulation period number, depth, and initial phase are investigated. With modulation period $n = 5$, modulation depth $K = 0.55$, and initial phase $\phi = 0$, cold atom clouds with more atom numbers, smaller final-vibration amplitude, and lower temperature are efficiently transported. Theoretical analysis and numerical simulation are also provided, which are in good agreement with experimental results.

Keywords: transport of cold atoms, modulation, velocity profile

PACS: 37.10.Vz, 37.10.Gh, 37.90.+j **DOI:** 10.1088/1674-1056/22/2/023702

1. Introduction

The transport of cold atoms is highly important in the experimental development in atomic physics. This process benefits experiments that require delivery of cold atoms on a set of experimental platforms separated by relatively long distances.[1–4] Cold atom transport also enables new applications of cold atoms, such as the usage as scan-probes to detect surfaces of several material structures.[5] Moreover, the transport of cold atoms itself is of significant interest,[6,7] as numerous phenomena accompanied by the transport still need to be reasonably explained.

Many approaches have been used to realize the transport of cold atoms. Neutral atoms have been transported by magnetic or optical traps.[8–14] Optical traps, such as optical tweezers, are used by mechanically moving the lenses to move the focal point[8–10] or by moving lattices realized with two counter-propagating beams.[1] Given the magnetic trap transport, scholars can mechanically move the coil,[2] vary the currents in a lithographic conductor pattern on the atom chip,[5] or use a conveyor belt that can be seen as a chain of magnetic trap dots.[3] In addition, the transport of ions in linear Paul traps[14] and an array of Penning traps[5] have been realized.

Usually, scholars choose a sufficiently slow and adiabatic transport[8,16,17] that is simple to realize without exciting the oscillation mode of the transported atom cloud mass center. However, in magnetic transport, the adiabatic process takes such a long time at a high energy cost. The long time required for the current to generate the magnetic trap sometimes results in unnecessary heating, which may induce magnetic field fluctuation and decoherence of ultra-cold atoms. In addition, adiabatic transport is impractical in many research studies, i.e., experiments must be completed in a short time in fast quantum information processing.[18,19] Considering the disadvantages of the slow, adiabatic approach, several theoretical and experimental studies on non-adiabatic methods have achieved fast, easy, and effective transport of cold atoms comparable to the ideal result of adiabatic transport.[6,7,20–22]

In this paper, non-adiabatic transport of cold atoms is investigated, and a lossless, fast transport with a final state close to the initial one is attempted. This method requires the transport to bring minimal heating as well as not to cause final vibration of the transported atoms mass center. Previous studies[6,7] report on some key factors that play important roles in avoiding these conditions. These factors include the velocity profile imposed on the transport trap,[6,7] and transport duration.

This study proposes to modulate the velocity profile imposed on the transport trap and experimentally demonstrates the proposal to optimize non-adiabatic transport of cold atoms. The rest of the present paper is organized as follows. In Section 2 a basic model for a transport process is introduced, and the amplitude of final vibration after the transport is analyzed to be the Fourier transform of the velocity profile. Two transport examples are compared, namely, using the velocity profile with and without modulation. The advantages of modulating the velocity profile are discussed in detail. In Section 3 the experiment is introduced and the results are discussed. An optimal transport of the cold ^{87}Rb atoms is obtained by modulating

*Project supported by the National Natural Science Foundation of China (Grant No. 10974210) and the National Basic Research Program of China (Grant No. 2011CB921504).

†Corresponding author. E-mail: zhanghc@siom.ac.cn

‡Corresponding author. E-mail: yzwang@mail.shcnc.ac.cn

© 2013 Chinese Physical Society and IOP Publishing Ltd

the velocity profile. The final-vibration amplitude dependence of the modulation parameters is also investigated. In Section 4 some conclusions are drawn from the present study.

2. Theory

2.1. Basic model

Assume that a neutral atom is being transported in one dimension by a magnetic trap potential, and let X denote the atom coordinate in the laboratory frame. The transport starts at time $t = 0$ and ends at $t = T$. Thus, the Newton's equation of motion[23] is

$$m\ddot{X}(t) = F, \tag{1}$$

where m is the atomic mass, and F is the force generated by the inhomogeneous magnetic field given by

$$F = -\frac{\partial E_B(X,t)}{\partial X}. \tag{2}$$

The above equation simply deals with a one-dimensional case. $E_B(X,t)$ is the potential energy of a neutral atom with magnetic moment $\boldsymbol{\mu}$ in a magnetic field $B(X,t)$, and expressed as

$$E_B(X,t) = -\mu \cdot B(X,t). \tag{3}$$

According to quantum mechanics, the projection of $\boldsymbol{\mu}$ on $B(X,t)$ has discrete values given by m_F, which is the quantum number of the component along the magnetic field direction of the total angular momentum $\boldsymbol{F} = \boldsymbol{I} + \boldsymbol{J}$. Here, $\boldsymbol{I}$ is the nuclear spin, and $\boldsymbol{J}$ is the total electron angular momentum. Therefore, the potential energy is

$$E_B(X,t) = g_F m_F \mu_B |B(X,t)|, \tag{4}$$

where μ_B is the Bohr magneton, and g_F is the Landé g-factor.

For a magnetic harmonic trap, the force is

$$F = -m\omega_0^2 [X(t) - X_c(t)], \tag{5}$$

where $X_c(t)$ is the trap center coordinate in a laboratory frame, and ω_0 is the frequency of the magnetic harmonic trap along the transport direction, and expressed as

$$\omega_0 = \sqrt{\frac{\mu}{m} B''}. \tag{6}$$

A magnetic quadrupole trap is used as the transport trap with a frequency that can be estimated as done in Ref. [24]. For simplicity, the transport trap is considered as a harmonic trap. Therefore, atom transport by a harmonic trap can be described by the motion equation,

$$\ddot{X}(t) + \omega_0^2 X(t) = \omega_0^2 X_c(t). \tag{7}$$

An arbitrary solution of this kind of differential equation with the initial condition $X(0) = 0, \dot{X}(0) = 0$ can be given by

$$X(t) = \omega_0 \int_0^t X_c(t') \sin[\omega_0 (t - t')] \, dt'. \tag{8}$$

A velocity profile $V_c(t)$, used as a function of time, is imposed on the transport trap

$$V_c(t) = \dot{X}_c(t) = v_c(t)[h(t) - h(t - T)]. \tag{9}$$

The unit step function $h(t)$ determines the transport duration from $t = 0$ to $t = T$,

$$h(t - t_0) = \begin{cases} 1, & t \geq t_0, \\ 0, & t < t_0. \end{cases} \tag{10}$$

The trap velocity is zero before transport starts ($t \leq 0$), as well as after the transport has ended ($t \geq T$). During the transport ($0 < t < T$), the velocity profile $V_c(t)$ changes into function $v_c(t)$.

Assuming that the initial position of the trap center is $X_c(0) = 0$, equation (8) can be simplified into

$$X(t) = X_c(t) - \int_0^t V_c(t') \cos[\omega_0 (t - t')] \, dt'. \tag{11}$$

After the transport, the trap is kept on, and the final vibration of the atom ($t > T$) is defined as

$$s(t) \equiv X(t) - X_c(t), \quad t > T. \tag{12}$$

Therefore,

$$s(t) = -\int_0^T V_c(t') \cos[\omega_0 (t - t')] \, dt', \quad t > T. \tag{13}$$

The final vibration $s(t)$ describes the atom oscillating around the trap center with the frequency of ω_0. The $s(t)$ can be expanded into the following form to infer the amplitude of the final vibration:[7]

$$\begin{aligned} s(t) &= -\cos(\omega_0 t) \int_0^T V_c(t') \cos(\omega_0 t') \, dt' \\ &\quad - \sin(\omega_0 t) \int_0^T V_c(t') \sin(\omega_0 t') \, dt' \\ &= C_1 \cos(\omega_0 t) + C_2 \sin(\omega_0 t) \\ &= A \cos[\omega_0 (t - T) + \varphi_T], \quad t > T. \end{aligned} \tag{14}$$

Here,

$$\begin{aligned} C_1 &= -\int_0^T V_c(t') \cos(\omega_0 t') \, dt', \\ C_2 &= -\int_0^T V_c(t') \sin(\omega_0 t') \, dt'. \end{aligned} \tag{15}$$

The final-vibration amplitude after the transport is

$$A = \sqrt{C_1^2 + C_2^2}, \tag{16}$$

and the phase φ_T at $t = T$ obeys

$$\cos(\omega_0 T - \varphi_T) = \frac{C_1}{\sqrt{C_1^2 + C_2^2}},$$
$$\sin(\omega_0 T - \varphi_T) = \frac{C_2}{\sqrt{C_1^2 + C_2^2}}. \quad (17)$$

Considering the property of the velocity profile shown in Eq. (9), C_1 and C_2 defined by Eq. (15) can be rewritten as

$$C_1 = -\int_{-\infty}^{+\infty} V_c(t') \cos(\omega_0 t')\, dt',$$
$$C_2 = -\int_{-\infty}^{+\infty} V_c(t') \sin(\omega_0 t')\, dt'. \quad (18)$$

Thus, the final-vibration amplitude and phase can be expressed as

$$A = \left| \mathscr{F}[V_c(t)]|_{\omega_0} \right|,$$
$$\varphi_T = \omega_0 T - \angle \mathscr{F}[V_c(t)]|_{\omega_0} - \pi, \quad (19)$$

where $\mathscr{F}[V_c(t)]$ is the Fourier transform of the velocity profile $V_c(t)$, i.e., $\mathscr{F}[V_c(t)] = \int_{-\infty}^{+\infty} V_c(t)\, e^{-i\omega t} dt$.

We must keep the final-vibration amplitude as small as possible to obtain a final state close to the initial one. The final-vibration amplitude A is not the distance between the atom and the trap center at $t = T$, expressed by $s(T) = X(T) - X_c(T)$. The value of A in Eq. (16) would be zero if and only if $C_1 = 0$ and $C_2 = 0$. From Eq. (14), when the phase part φ_T happens to be $(N + 1/2)\pi$ (N is an integer), the distance $s(T)$ would be zero, whereas A would still exist. Equations (11) and (13) indicate that the atom would not exactly follow the center of the harmonic trap, and would instead oscillate around the trap center during transport. At the end of the transport, the atom may stay in the trap center, and as such, retain velocity. In such a case, after the trap stops, the atom still oscillates around its center. Only when the atom stays in the trap center with zero velocity, will its oscillation stop. The velocity profile with a low or zero amplitude of ω_0 component will be a good choice for non-adiabatic transport.

2.2. Example: using a square velocity profile

Assume that the frequency of the harmonic trap $\omega_0 = 2\pi \times 16$ Hz, transport distance $L = 22$ mm, and duration $T = 200$ ms, the square velocity profile will be written as a function of time (shown in Fig. 1(a)):

$$V_c(t) = \frac{L}{T}[h(t) - h(t - T)], \quad (20)$$

where $v_c(t) = L/T$ is a constant.

The frequency properties of the velocity profile (shown in Fig. 1(b)) provide information about the final-vibration amplitude. The frequency component $\omega_0 = 2\pi \times 16$ Hz has a relatively large magnitude. Thus, according to Eq. (19), the final-vibration amplitude brought about by the square velocity profile will be as large as 0.5 mm.

The motion trajectory of the atom (Fig. 1(c)) directly shows the vibration. Equation (7) is numerically simulated using the velocity profile expressed in Eq. (20). The initial condition is set to be $X(0) = 0$, $\dot{X}(0) = 0$, and $X_c(0) = 0$. After transport, the trap velocity becomes zero, and the trap is kept on for 200 ms. Thus, the total simulated time is $t_f = T + 200$ ms. The square velocity profile imposed on the transport trap causes a large final-vibration amplitude.

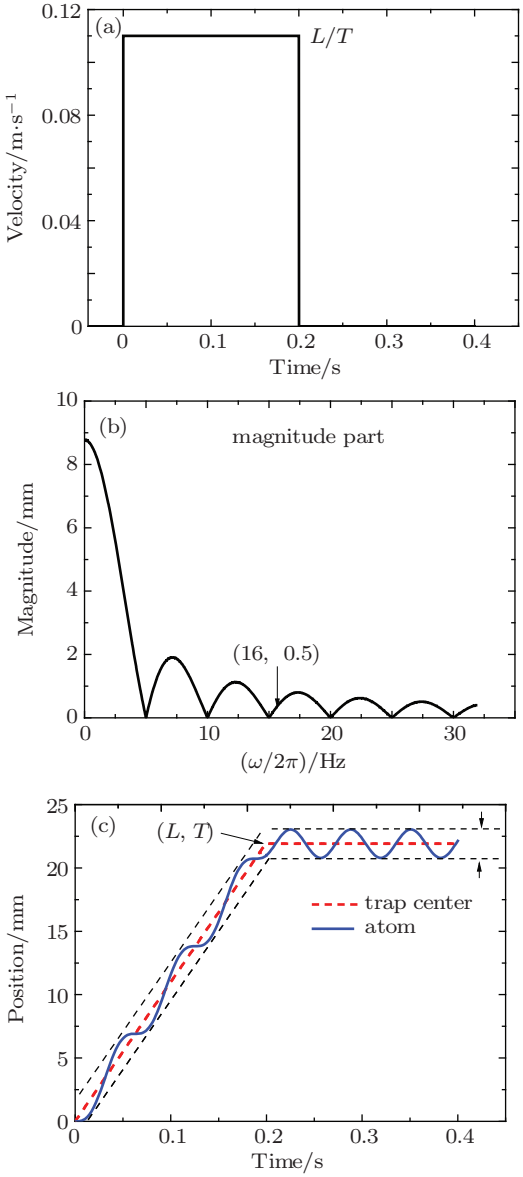


Fig. 1. (color online) (a) Square velocity profile imposed on the trap; (b) magnitude part of the Fourier transform for the velocity profile; (c) simulation for the motion trajectory of the atom and trap center. The dashed and solid lines represent the motion trajectories of the trap center $X_c(t)$ and the atom $X(t)$, respectively. Transport distance $L = 22$ mm; transport duration $T = 200$ ms; trap frequency $\omega_0 = 2\pi \times 16$ Hz.

From Fig. 1(b), the amplitude curve has some zero values. The trap frequency with zero amplitude can be chosen to

obtain fast transport without final vibration. Similarly, special transport duration may be chosen. However, the curve around those zero points would be very sharp, indicating that this kind of transport is highly sensitive to the trap frequency or transport duration. A small fluctuation in the magnetic field would cause a large vibration. Keeping trap frequency constant is difficult in experiments, and thus, this kind of transport would cause splitting of the cold atom cloud and bring in a significant heating effect.

2.3. Example: modulating the velocity profile

The velocity profile with modulation is used to lower the final-vibration amplitude with frequency component ω_0

$$V_{\rm c}(t) = \frac{L}{T}\left[1+K\cos\left(\frac{2\pi nt}{T}+\varphi\right)\right][h(t)-h(t-T)], \quad (n=1,2,3,\ldots,\ 0\le K\le 1,\ -\pi\le\varphi\le\pi), \quad (21)$$

where

$$v_{\rm c}(t) = \frac{L}{T}\left[1+K\cos\left(\frac{2\pi nt}{T}+\varphi\right)\right],$$

L is the transport distance, T is the transport duration, K is the modulation depth, φ is the initial phase of the modulation, and n is the period number of cosine modulations added to the velocity profile. The n is kept as an integer to ensure that the integration of velocity over the transport duration is the transport distance L.

Assuming that the transport is done under the same condition as those in Subsection 2.2, except for the modulated velocity profile (shown in Fig. 2(a)), figure 2(b) shows the frequency components of the velocity profile. Obviously, the magnitude of the frequency component ($\omega_0 = 2\pi\times 16$ Hz) is successfully lowered to 0.02 mm upon adding four periods of cosine modulation with depth $K = 0.55$ and initial phase $\varphi = 0$ (shown in Fig. 2(a)). According to Eq. (19), the final-vibration amplitude is lowered.

Figure 2(c) directly shows the reduced final-vibration amplitude through velocity profile modulation. Equation (7) is numerically simulated using the velocity profile expressed in Eq. (21) with $K = 0.55$, $\varphi = 0$, and $n = 4$ (shown in Fig. 2(a)). The initial condition is set to be $X(0) = 0$, $\dot{X}(0) = 0$, and $X_{\rm c}(0) = 0$. The numerical simulation is in good agreement with the frequency analysis: by modulating the velocity profile imposed on the trap, the atom has a very small final vibration.

Figure 2(b) shows the curve having a flat area where amplitude is nearly zero. The transport of cold atoms with a modulated velocity profile is insensitive to trap frequency or transport duration. Due to the appealing property of this method, the heating or splitting of the cold atom cloud during transport in a magnetic quadrupole trap may be avoided.

Final-vibration amplitude depends strongly on these modulation parameters: depth, initial phase, and period number (shown in Fig. 3). These parameter effects are considered in the numerical simulation. Figure 3(a) infers the final-vibration amplitude dependence of the modulation period number n, keeping $K = 0.55$, $\varphi = 0$. The n=0 means that the velocity profile without modulation is used. Similarly, figure 3(b) (Fig. 3(c)) shows the final-vibration amplitude dependence of the modulation depth (initial phase of modulation). When adding four periods of cosine modulation with $K = 0.55$ and $\varphi = 0$, the amplitude final-vibration amplitude is the smallest value (see points A, B, and C in Fig. 3).

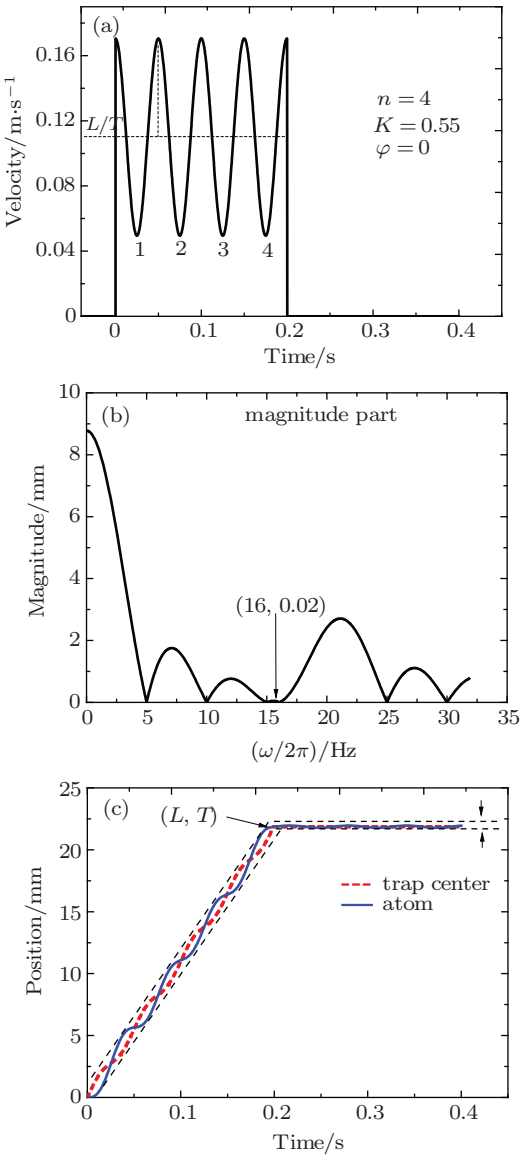


Fig. 2. (color online) (a) Velocity profile with modulation; (b) magnitude part of the Fourier transform for the velocity profile; (c) simulation for the motion trajectory of the atom and trap center. The dashed and solid lines show the motion trajectory of the trap center $X_{\rm c}(t)$ and the atom $X(t)$, respectively. The conditions are the same as those in Subsection 2.2, except for the velocity profile with modulation depth $K = 0.55$, initial phase $\varphi = 0$, and the period number of cosine modulation $n = 4$.

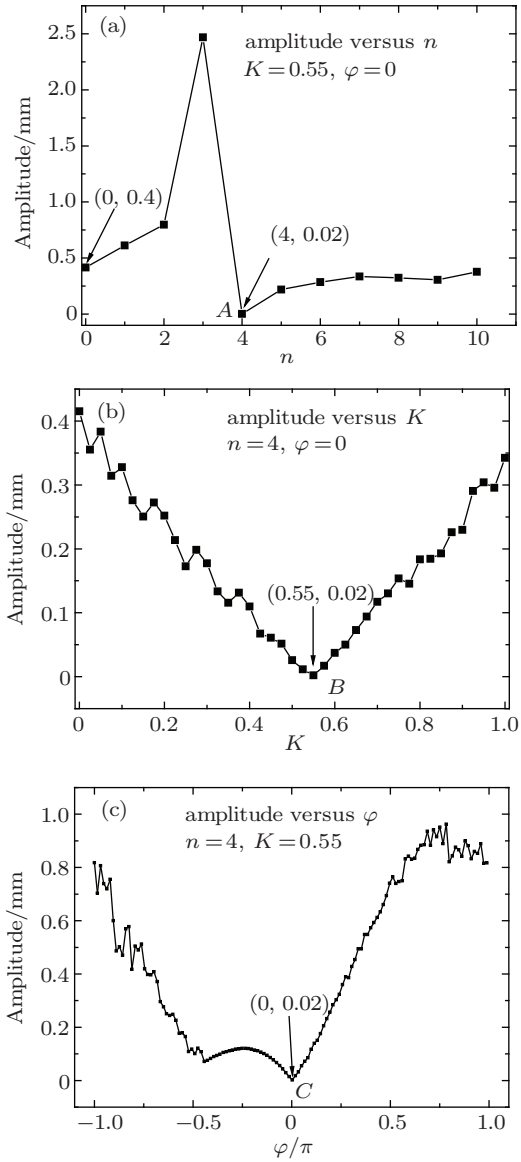


Fig. 3. Numerical results for final-vibration amplitude. (a) Amplitude dependence of modulation period number n, with $K = 0.55$ and $\varphi = 0$; (b) amplitude dependence of modulation depth K, with $n = 4$ and $\varphi = 0$; (c) amplitude dependence of modulation initial phase φ, with $n = 4$ and $K = 0.55$.

2.4. Discussion

The final-vibration amplitude of transported atoms becomes small through several methods, such as adiabatic transport with long transport duration T.[8,16,17] However, some disadvantages cannot be avoided, including impracticality in some experiments.[8,19] Another way is to choose a special transport trap frequency ω_0 or transport duration T[6] to achieve fast transport without final vibration. When using a different method, the trap frequency should be highly stable during the transport, because the curve is very steep around the zero points (shown in Fig. 1(b)), and therefore sensitive to transport duration or trap frequency. In experiments, this method would cause the splitting of a cold atom cloud and bring about a significant heating effect as mentioned earlier.

Modulating the velocity profile to obtain a small final-vibration amplitude is especially appealing when the transport trap frequency is not rigid, for example, a magnetic quadrupole trap. Figure 2(b) shows that the curve is very flat around the trap frequency ω_0. In other words, the amplitude remains very small in a large area in the frequency domain around ω_0. This indicates that a small variation in trap frequency would not cause a large final-vibration amplitude. Another advantage of the proposed method is that the transport duration should be invariable in some experiments;[5] by modulating the velocity profile, the final-vibration amplitude of transported atoms can be lowered without changing the transport duration.

3. Experiment

3.1. Experimental setup and process

Cold ^{87}Rb atoms are experimentally transported under nearly similar conditions with the previous numerical simulation, to demonstrate that modulating trap velocity can be used to optimize the transport of cold atoms. The target distance is $L = 22$ mm, and the transport duration is $T = 200$ ms. Figure 4 shows the major experimental setup in this work. Two pairs of anti-Helmholtz coils, MOT, and transfer coil pair, partly overlap. The centers of these coil pairs are vertically separated by 40 mm. Cold atoms can be transported along the gravitational direction. The currents of the two coil pairs are varied to move the magnetic quadrupole potential trap. The velocity profile imposed on the trap is modulated as expressed in Eq. (21). An optimal condition for transport is obtained through the variations of modulation parameters.

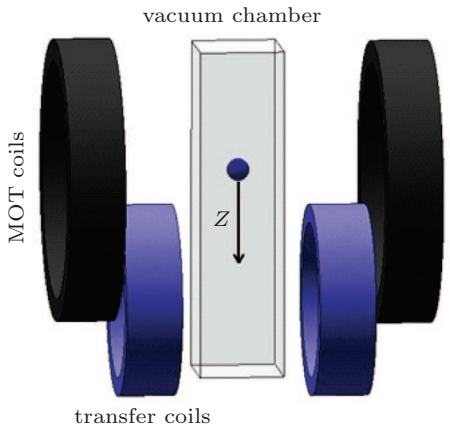


Fig. 4. (color online) Schematic plot of the experimental setup.

The frequency of the quadrupole potential trap is estimated by the method used in Ref. [24]. As stated, a cloud of size r is assumed to be in a linear potential with gradient B'. Then, the cloud would be confined to the same size in a parabolic potential with a curvature of B'/r. An effective curvature of linear confinement is defined as $B''_{\rm eff} = B'_{\rm coil}/r$, and the effective trap frequency is defined as $\omega_{\rm eff} = \sqrt{\mu B''_{\rm eff}/m}$.

In the experiment, frequency varies with transport distance increasing. The trap depth in the transport process is in a range from 6 mK to 10 mK. Concurrently, the frequency is $2\pi \times 9$ Hz at the beginning of the transport process, and $2\pi \times 19$ Hz at the end. The average frequency of the trap over the distance from 0 mm to 22 mm is $2\pi \times 16$ Hz.

The transport of cold atoms is conducted as follows. First, a typical MOT setup is used to produce cold atoms. Then, polarization gradient cooling is performed by turning off the magnetic trap, reducing the power intensity, and linearly increasing the detuning of MOT beams. After that, the atoms are optically pumped into $|F = 2, m_F = 2\rangle$ state of ground level $5^2S_{1/2}$ with the bias field 4 Gs (1 Gs=10^{-4} T). Next, the magnetic potential trap is switched on with a radial gradient of 20 Gs $\cdot$ cm^{-1} for 7 ms to load the atoms into the quadrupole trap and start the transport. Afterward, the number of loaded atoms is about 6×10^6 with a density of 1.7×10^6 mm^{-3}, and the temperature of the cold atom cloud is about 130 μK. A modulated velocity profile with different parameters is used to move the magnetic quadrupole potential trap downward over a distance of 22 mm from the MOT center.

Standard fluorescence imaging technique is used on a charge-coupled device camera to record the images of the cold atom cloud. When the magnetic quadrupole trap is turned off at the end of the transport, a circularly polarized laser pulse is used as the probe light with an intensity of 2.4 mW $\cdot$ cm^{-2} and a duration of 1 ms. The laser pulse is red-detuned by 13 MHz compared with the pulse from the $5^2S_{1/2}(F = 2) \rightarrow 5^2P_{3/2}(F' = 3)$ transition. For each image, the transport process is conducted once due to the destructive imaging process. The scope of the atom cloud is specified within e^{-1} folding the highest fluorescence intensity for calculating the atom number. The time-of-flight probing technique is used for temperature measurement. For the final-vibration amplitude of the transported atom mass center, the trap is kept on and the position of the atom cloud mass center is measured every 5 ms from 0 ms to 50 ms by recording a set of images after the transport for different modulations.

3.2. Results and analyses

Figure 5 shows the results of the present experiment. The final-vibration amplitude dependences of modulation period number, depth, and initial phase are investigated through experiments. In Fig. 5(a), $n = 0$ means that the velocity profile is applied without modulation. The experimental results are in good agreement with the numerical simulations. Using the velocity profile without modulation causes the atom mass center to vibrate with amplitude equal to 1.16 mm. When modulating the velocity profile with period number $n = 5$, depth $K = 0.55$, and initial phase $\varphi = 0$, the final-vibration amplitude is lowered to 0.46 mm. The final-vibration amplitude provides information about heating and excitation caused by the transport. A small amplitude implies an efficient transport with lower atomic temperature and larger atomic number. Figure 6 shows the atomic temperature and number dependence of the modulation period number.

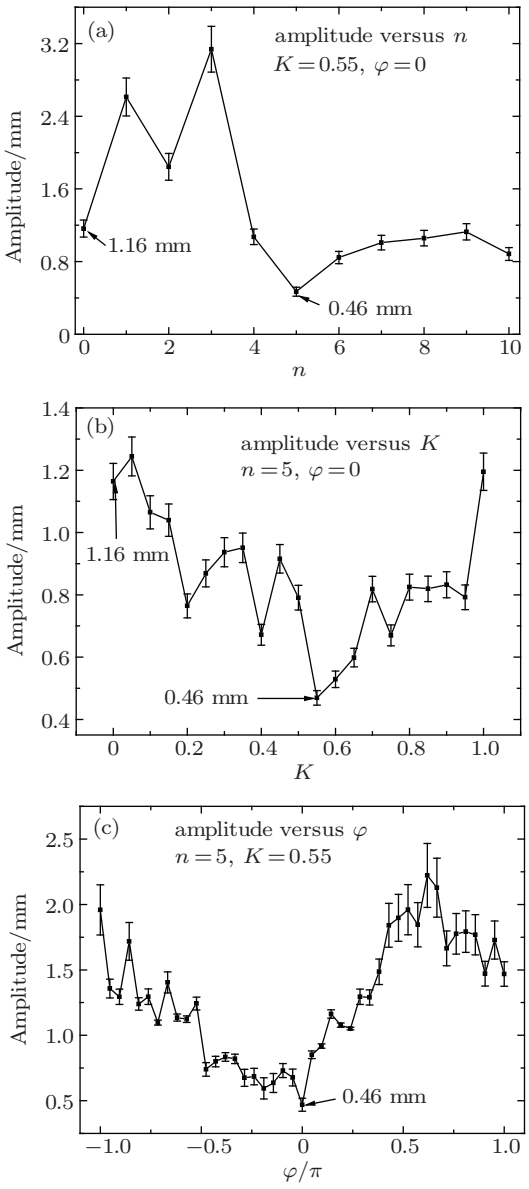


Fig. 5. Measured final-vibration amplitudes. (a) Amplitude dependence of modulation period number n, with $K = 0.55$ and $\varphi = 0$; (b) amplitude dependence of modulation depth K, with $n = 5$ and $\varphi = 0$; (c) amplitude dependence of modulation initial phase φ, with $n = 5$ and $K = 0.55$.

In Fig. 6, in the absence of modulation, the transported atom number is about 3.5×10^6 and the temperature is about 330 μK. When adding modulation with period number $n = 5$, depth $K = 0.55$, and initial phase $\varphi = 0$, the transported atom number is about 4.5×10^6 and temperature is as low as 190 μK. In the experiment, the number of loaded atoms before transport is about 6×10^6, with temperature about 130 μK. Thus, by modulating the velocity function, efficiency increases from 58% to 75%, whereas the temperature reduces from

330 μK to 190 μK.

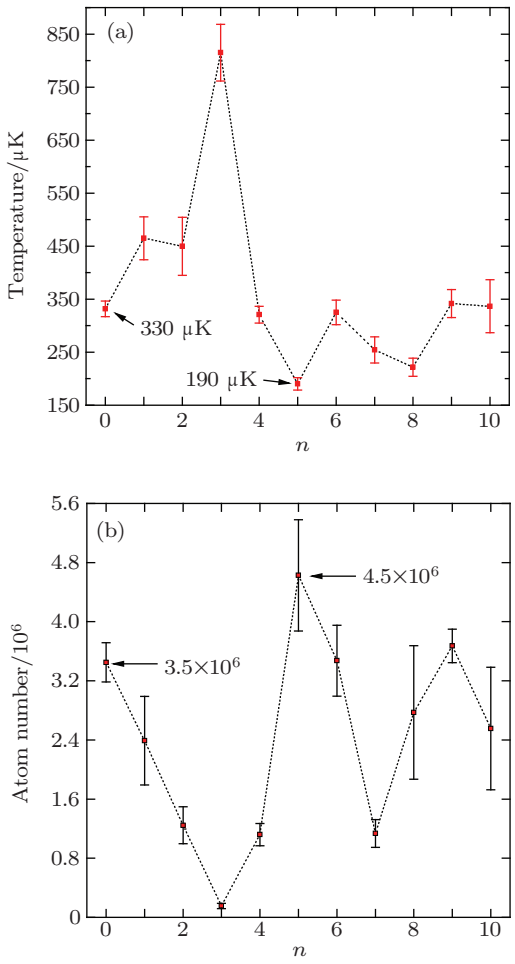


Fig. 6. (color online) Measured dependences temperature of transported atoms (a) and atom number (b) on modulation period number, with the modulation depth $K = 0.55$ and initial phase $\varphi = 0$. Here, $n = 0$ means that the transport uses the velocity profile without modulation.

The experimental results are slightly different from the numerical simulations, showing that the final-vibration amplitude is the smallest when adding modulation with period number $n = 4$, depth $K = 0.55$, and initial phase $\varphi = 0$ modulation on the velocity profile. However, the values $n = 5$, $K = 0.55$, and $\varphi = 0$ are used in the experiment. This may be caused by changing the trap frequency in the transport process. The trap frequency is rigid in the simulation but changing in the experiment. Moreover, a harmonic trap is used in the numerical simulation, but a magnetic quadrupole trap is used in the experiment. Transport with a modulated velocity profile successfully lowers the final-vibration amplitude as it is insensitive to trap frequency.

4. Conclusions

In this work a non-adiabatic transport of cold atoms in a magnetic quadrupole trap is optimized by modulating the velocity of the trap potential. When selecting a proper modulation period n, depth K, and initial phase φ, the final-vibration amplitude should remain very small over a large range in the frequency domain. Thus, the heating effect is reduced. Several special transport durations[6] are chosen to obtain a non-adiabatic transport without final vibration. However, this kind of transport, free of modulation, is sensitive to trap frequency or transport duration, because its amplitude curve around each of the zero points is very sharp. This may cause splitting of the atom cloud and lead to a significant heating effect. Optimizing transport by modulating the trap potential velocity can avoid such problems as it is insensitive to the trap frequency or transport duration. This method works not only in experiments where a magnetic trap is used to transport cold atoms, such as a magnetic quadrupole trap, but also in experiments using an optical trap.

References

[1] Cirac J I, Zoller P, Kimble H J and Mabuchi H 1997 *Phys. Rev. Lett.* **78** 322

[2] Sauer J A, Fortier K M, Chang M S, Hamley C D and Chapman M S 2004 *Phys. Rev.* A **69** 051804

[3] Colombe Y, Steinmetz T, Dubois G, Linke F, Hunger D and Reichel J 2007 *Nature* **450** 272

[4] Greiner M, Bloch I, Hänsch T W and Esslinger T 2001 *Phys. Rev.* A **63** 031401

[5] Gierling M, Schneeweiss P, Visanescu G, Federsel P, Häffner M, Kern D P, Judd T E, Günther A and Fortágh J 2011 *Nature Nanotechnology* **6** 446

[6] Chen D Y, Zhang H C, Xu X P, Li T and Wang Y Z 2010 *Appl. Phys. Lett.* **96** 134103

[7] Couvert A, Kawalec T, Reinaudi G and Guéry-Odelin D 2008 *Europhys. Lett.* **83** 13001

[8] Gustavson T L, Chikkatur A P, Leanhardt A E, Görlitz A, Gupta S, Pritchard D E and Ketterle W 2001 *Phys. Rev. Lett.* **88** 020401

[9] Prestage J D, Tjoelker R L, Dick G J and Maleki L 1993 *Proceedings of the* 1993 *IEEE Frequency Control Symposium*, June 2–4 1993, Salt Lake City, USA, p. 144

[10] He J, Yang B D, Zhang T C and Wang J M 2011 *Chin. Phys.* B **20** 073701

[11] Kuhr S, Alt W, Schrader D, Dotsenko I, Miroshnychenko Y, Rosenfeld W, Khudaverdyan M, Gomer V, Rauschenbeutel A and Meschede D 2003 *Phys. Rev. Lett.* **91** 213002

[12] Lewandowski H J, Harber D M, Whitaker D L and Cornell E A 2003 *J. Low Temp. Phys.* **132** 309

[13] Lahaye T, Reinaudi G, Wang Z, Couvert A and Guéry-Odelin D 2006 *Phys. Rev.* A **74** 033622

[14] Huber G, Deuschle T, Schnitzler W, Reichle R, Singer K and Schmidt-Kaler F 2008 *New J. Phys.* **10** 013004

[15] Crick D R, Donnellan S, Ananthamurthy S, Thompson R C and Segal D M 2010 *Rev. Sci. Instrum.* **81** 013111

[16] Hänsel W, Hommelhoff P, Hänsch T W and Reichel J 2001 *Nature* **413** 498

[17] Schrader D, Kuhr S, Alt W, Müller M, Gomer V and Meschede D 2001 *Appl. Phys.* B **73** 819

[18] Rowe M A, Ben-Kish A, DeMarco B, Leibfried D, Meyer V, Beall J, Britton J, Hughes J, Itano W M, Jelenkovic B, Langer C, Rosenband T and Wineland D J 2002 *Quantum Inf. Comput.* **4** 257

[19] Lau H K and James D F V 2001 *Phys. Rev.* A **83** 062330

[20] Chen Xi, Torrontegui E, Dionisis S, Li J S and Muga J G 2011 *Phys. Rev.* A **84** 043415

[21] Torrontegui E, Ibáñez S, Chen Xi, Ruschhaupt A, Guéry-Odelin D and Muga J G 2011 *Phys. Rev.* A **83** 013415

[22] Torrontegui E, Chen X, Modugno M, Schmidt S, Ruschhaupt A and Muga J G 2012 *New J. Phys.* **14** 013031

[23] Reichle R, Leibfried D, Blakestad R B, Britton J, Jost J D, Knill E, Langer C, Ozeri R, Seidelin S and Wineland D J 2006 *Fortschr. Phys.* **54** 666

[24] Ketterle W, Durfee D S and Stamper-Kurn D M 1999 *Bose–Einstein Condensation in Atomic Gases* (Amsterdam: IOS) p. 12